



OPEN Molecular dynamics simulations involving different β -propeller mutations reported in Swiss and French patients correlate with their disease phenotypes

Finola Priyadharshini Chandrasekaran & Everette Jacob Remington Nelson

Integrin α Ib β 3 is the predominant receptor for fibrinogen which mediates platelet aggregation, an important step in hemostasis and thrombosis. Several mutations have been reported in the genes encoding α Ib and β 3 subunits among patients with Glanzmann thrombasthenia, of which 177 are in the β -propeller domain. The two subunits form a heterodimer at the interface between β -propeller and β -I domains of α Ib and β 3, respectively with their stability critical for intracellular trafficking, surface expression, and ligand binding. Our study was aimed at retrieving the β -propeller mutations from various databases and studying structural variations due to select mutations upon interaction with fibrinogen using molecular docking and molecular dynamics. Mutations were studied for their impact on phenotypic severity, structural stability, and evolutionary conservation. Molecular docking analysis and molecular dynamics simulations were carried out for α Ib- β 3 complexes as well as α Ib β 3-fibrinogen complexes; in particular, E355K structure had more deviations, fluctuations, and other changes which compromised its structural stability and binding affinity when compared to both wild-type and G401C structures. Our comprehensive *in silico* analysis clearly reiterates that mutations in the β -propeller are not only responsible for structural changes in this domain but also have implications on the overall structure and function of integrin α Ib β 3.

Keywords α Ib β 3, β -propeller, Missense mutations, Molecular docking, Molecular dynamics, Glanzmann Thrombasthenia

Absent or abnormal surface expression or ligand binding of integrin α Ib β 3 results in an inherited bleeding disorder called Glanzmann thrombasthenia (GT). Hemostasis which refers to a physiological mechanism that arrests bleeding following injury to a blood vessel occurs in two phases: primary and secondary. Primary hemostasis as well as pathologic thrombosis (blood clot formation) is initiated by small, enucleated blood cells called platelets. Platelets recruited to the site of a ruptured blood vessel undergo adhesion (to vessel wall) and aggregation (to each other). Integrin α Ib β 3 is the predominant receptor for mediating platelet aggregation transitioning from a low-to-high affinity state for binding with fibrinogen and other ligands in response to soluble agonists (inside-out signaling). Ligand binding triggers integrin clustering leading to platelet spreading, irreversible aggregation, and clot retraction (outside-in signaling). Fibrinogen binding regions are localized to the N-terminal portions of integrin α Ib β 3. The upper face of the ectodomain constituting the headpiece of integrin α Ib β 3 has β -propeller and β -I domains that contain ligand binding sites (Fig. 1)¹. The β -propeller maintains stability of the protein structure of α Ib β 3 which is attributed to β -sheets in its secondary structure. The β -propeller structure consists of seven blades arising from consecutive amino acid repeats each of which includes 4 antiparallel strands with Ca^{2+} ions in every blade². While blades 1–3 are essential for associating with the β -I domain of β 3, blades 4–7 do not seem to have much importance albeit the presence of Ca^{2+} ions. In addition, the β -propeller has seven FG-GAP repeats of about 60 amino acids harboring putative Ca^{2+} binding motifs³.

The β -propeller domain is important for biogenesis, defects in which have often been associated with GT types 1 and 2. N15-linked glycosylation in the β -propeller was reported to control pro- α Ib maturation,

Gene Therapy Laboratory, Department of Integrative Biology, School of Bio Sciences and Technology, Vellore Institute of Technology, Vellore 632 014, India. email: aybegumkalyoncu@gmail.com

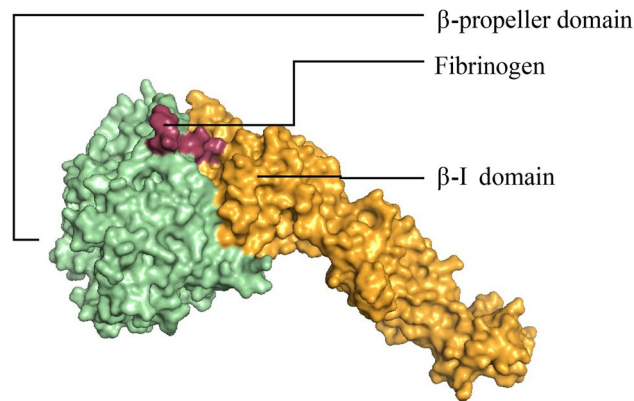


Figure 1. Depiction of fibrinogen (γ C peptide) interacting domains of α IIb β 3⁴.

heterodimerization, and degradation⁵. The N15-glycated pro- α IIb heterodimerizes with β 3 in the endoplasmic reticulum (ER) which is followed by carbohydrate modification and proteolytic cleavage in the Golgi apparatus to form mature α IIb β 3 complexes⁶. Mutations in the β -propeller were found to abrogate complex formation thereby preventing their transport from the ER to Golgi, which implies the intricate role of this domain^{7–12}. Structural modifications caused by the mutations G128S, S287L, and G357S that variably impaired progression of pro- α IIb β 3 complexes from the ER to Golgi were characterized in our previous study¹³.

Integrin α IIb β 3 is capable of binding to ligands, such as fibrinogen, fibrin, von Willebrand factor, and fibronectin. Fibrinogen is a physiologically important ligand that is involved in crosslinking activated platelets, a vital step in hemostasis. The binding event happens between the γ -C peptide in fibrinogen and interface of the “cap” region containing 4 loops on the top side of the α IIb β -propeller domain and “specificity determining loop” in the β 3 β -I domain¹⁴. The ligand binding sites require Ca^{2+} and Mg^{2+} ions for proper binding of α IIb and β 3 subunits. Most of the Ca^{2+} ions are located on the blades of β -propeller determining the stability and folding of the structure. The residues 1–334 of the β -propeller were reported to regulate fibrinogen binding. Earlier, peptide crosslinking residues 171–464 and 294–314 in recombinant α IIb highlighted the importance of these residues in ligand binding. Most of the naturally occurring mutations involving the residues 145–224 of the β -propeller affected ligand binding¹⁵.

In particular, mutations in the residues 184–193 of the third amino terminal repeat blocked fibrinogen binding¹⁶. Among them, D163A was found to affect ligand binding by causing a defect in folding, while T176I, Y143H, and P145A^{4,16} also led to a failure in binding with fibrinogen. Most of the GT mutations reported so far are associated with the β -propeller domain, which shows its indispensable contribution to the structure and function of the integrin α IIb β 3. The aim of this study was to retrieve missense mutations in this domain from various databases and highlight structural changes due to select mutations upon interaction with fibrinogen using molecular docking and molecular dynamics.

Results

Mutation screening

A total of 177 single nucleotide polymorphisms (SNPs) obtained from the various databases were located within amino acid residues 1–451 of the α IIb subunit corresponding to the β -propeller domain (Table S1).

Pathogenicity analysis

All identified SNPs were further analyzed for their pathogenicity using PredictSNP¹⁷, out of which sixty were predicted to be deleterious and pathogenic using tools, such as PredictSNP, MAPP, PhD-SNP, Polyphen-1, Polyphen-2, SIFT, and SNAP (Table S2). Not surprisingly, most of these mutations that were associated with specific functional defects correlated with GT type 1.

Stability analysis

Mutations affecting the structural stability of a protein are often responsible for the disease phenotype. Hence, mutations with deleterious and pathogenic consequences were studied further. These mutations were analyzed for their impact on structural stability using the iStable¹⁸ tool, which is used for analyzing the changes in stability as a result of the mutations. Twenty-seven mutations were found to destabilize the structure of integrin α IIb β 3 based on the DDG scores obtained using tools, like MuPro, iStable and I-Mutant (Table S3).

Conservation analysis

Amino acid residues that are highly conserved during the course of evolution are unlikely to be mutated. Accordingly, conservation analysis was done for all the identified mutations and only those that involved highly conserved residues were studied further. Nine mutations had occurred in highly conserved regions as indicated (Fig. 2A). Among these, while residues G44, E355, and G401 are highly conserved and exposed on the β -propeller surface, residues P176, G267, G296, and G321 although highly conserved, are buried. The

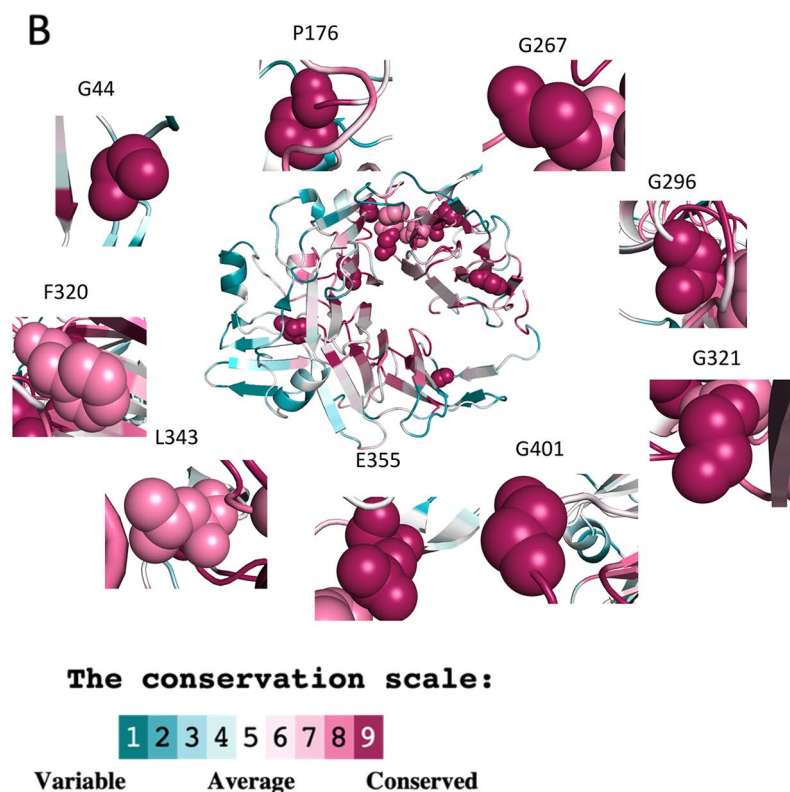
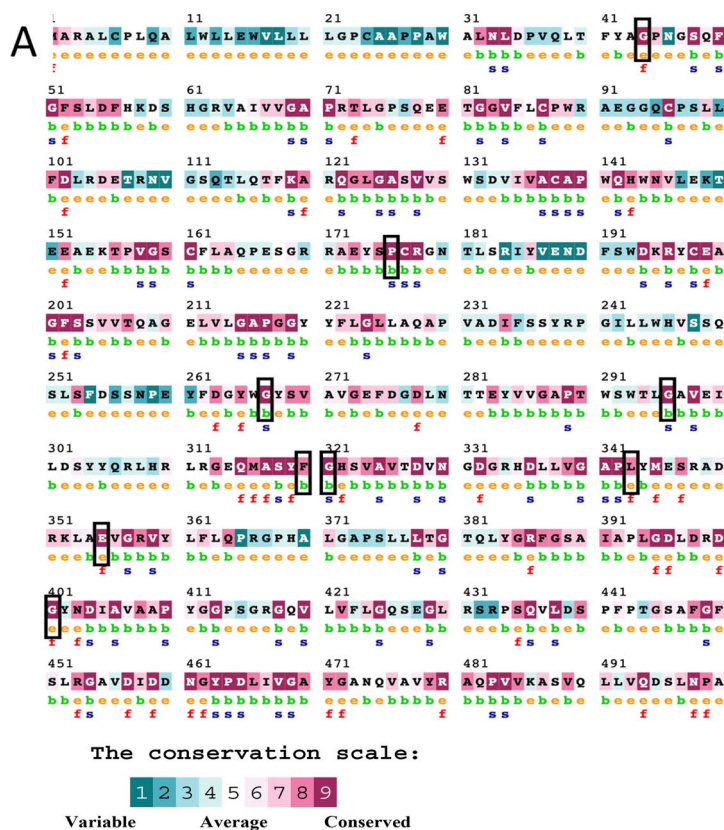


Figure 2. Evolutionary conservation analysis of the α IIb amino acid sequence (A) with the highly conserved amino acid residues depicted on the β -propeller structure (B).

other residues, namely F320 and L343 are also conserved and buried (Fig. 2B). Although these mutations were reported to be functionally important, structural changes caused by them have not been studied in detail.

Molecular docking studies

Some of the prominent and functionally significant mutations reported in the literature were chosen for this study (Table 1). The wild-type, G296R, F320S, G321W, E355K, and G401C α IIB β 3 structures were subjected to molecular docking analysis, which revealed the binding energy, docking score, and binding orientation between the α IIB and β 3 subunits (Table 2). In general, mutant structures with lower binding energies were found to form highly stable complexes with greater binding affinity. Among the five mutations, E355K and G401C had the highest binding energies indicating that these two mutations might affect fibrinogen binding to mutant α IIB β 3 complexes when compared to the wild-type due to changes in the interactions (Fig. 3A–C). Therefore, E355K and G401C mutations were considered for MD simulations to better understand their deleterious consequences as detailed below.

MD trajectory analysis

E355K compromised stability as compared to G401C

RMSD was calculated to determine the convergence and deviations with time based on Ca atoms in the wild-type, E355K, and G401C α IIB β 3 structures bound to fibrinogen (Fig. 4A). The average RMSD values of E355K and G401C α IIB β 3 complexes with fibrinogen were observed to be higher as compared to that of the wild-type (Table 3). The protein structures were stabilized with fixed values which indicated that the docked complexes of E355K and G401C had deviations throughout the simulation period (500 ns), with E355K recording the highest fluctuation. Similarly, RMSF was calculated which indicated the changes in flexibility of the wild-type, E355K, and G401C α IIB β 3 structures over time when bound with fibrinogen. The E355K structure displayed more flexibility implying stability changes when compared to the wild-type, with the G401C structure showing slightly less fluctuation (Fig. 4B). The average RMSF values of E355K and G401C α IIB β 3 complexes with fibrinogen were observed to be higher as compared to that of the wild-type (Table 3).

The Rg value of a protein structure is used to calculate the distribution of atoms from the centre of the mass, which denotes the compactness of the protein structure. The competence and folding of the wild-type, E355K, and G401C α IIB β 3 structures bound to fibrinogen were observed at different time points during the trajectory, which revealed that when compared to the wild-type fibrinogen-bound α IIB β 3 complex, both E355K and G401C complexes exhibited more deviations thereby compromising the compactness of the protein structure (Fig. 5A). The average Rg values of fibrinogen-bound wild-type, E355K, and G401C α IIB β 3 complexes were 3.83, 4.31, and 4.11 nm, respectively (Table 3). SASA was performed in order to identify the changes caused by mutations in the hydrophobic core of the protein structure, which showed changes in SASA associated with both fibrinogen-bound E355K and G401C complexes as compared to the wild-type (Fig. 5B). The average SASA values of fibrinogen-bound wild-type, E355K, and G401C α IIB β 3 complexes were 673.33 +/- 29.10, 746.03 +/- 15.69 and 718.12 +/- 16.48, respectively (Table 3). An increase or decrease in the SASA values is indicative of an impact on the protein structure. Accordingly, the E355K mutation with a higher SASA value resulted in an enlarged solvent-accessible surface area in the E355K structure.

Compactness and flexibility of the protein structure are reciprocally connected to each other. Rg and SASA were calculated to study the accessible surface area of mutant structures for the solvent. Kernel density estimation plots of Rg and SASA for wild-type, E355K, and G401C α IIB β 3 structures were plotted, which revealed significant differences in the mutant structures when compared to the wild-type (Fig. 6).

Intermolecular H-bond

The hydrogen bonds present in a protein are responsible for maintaining its structure and determining its binding specificity. Intermolecular hydrogen bonds were observed with respect to the wild-type, E355K, and G401C α IIB β 3 structures bound to fibrinogen which indicated changes in interactions after 350 ns in the mutant complexes when compared to the wild-type (Fig. 7).

Secondary structure elements

Mutations causing changes to the secondary structure of the fibrinogen-bound wild-type and mutant α IIB β 3 complexes were evaluated. The structural behavior of a protein may be influenced by the proportion of secondary structure elements, like α -helixes, β -sheets, turns, etc. Overall, the E355K and G401C complexes had slightly more of these structures, mainly β -sheets, when compared to the wild-type (Table 4).

E355K affected fibrinogen binding

Binding free energy was calculated using the molecular mechanics Poisson-Boltzmann surface area (MM-PBSA) approach to study the energy association between the α IIB β 3 and fibrinogen structures throughout the MD simulation period. Although the average binding energies for the E355K and G401C structures were found to be lower when compared to the wild-type structure (Table 5A), binding energies associated with active residues involved in ligand binding were higher for these mutant structures when compared to that of the wild-type (Table 5B). Table 5 was divided into parts a and b. It is important that tables are numbered in ascending numerical order: 1, 2, and 3. Since such table cannot be separated because of a main caption, it was merged and referred as Table 5. Please check if the modified presentation is appropriate. Otherwise kindly advise us on how to proceed.

Accession number	Mutation	I-Mutant	MUpro	I-Stable	PredictSNP	MAPP	PhD-SNP	PolyPhen-1	PolyPhen-2	SIFT	ConSurf	Refs.
CM061068	G296R	D	D	D	D	D	D	D	D	D	8	19
CM153672	F320S	D	D	D	D	D	D	D	D	D	9	20
CM030472	G321W	D	D	D	D	D	D	D	D	D	9	34
CM981073	E355K	D	D	D	D	D	D	D	D	D	9	35
CM153663	G401C	D	D	D	D	D	D	D	D	D	9	34

Table 1. Prominent β -propeller mutations causing Glanzmann thrombasthenia. D – Deleterious / Destabilizing

Protein structure	HADDOCK score	Van der Waals energy	Electrostatic energy
Wild-type	-59.0 +/- 28.9	-66.0 +/- 9.8	-371.3 +/- 92.5
G296R	-163.4 +/- 4.4	-83.6 +/- 5.1	-391.8 +/- 28.1
F320S	-139.7 +/- 4.2	-100.3 +/- 16.6	-423.8 +/- 65.6
G321W	-177.3 +/- 35.2	-102.0 +/- 12.3	-569.8 +/- 91.5
E355K	-60.0 +/- 38.9	-76.0 +/- 10.8	-361.3 +/- 136.5
G401C	-124.3 +/- 42.5	-85.0 +/- 20.7	-687.0 +/- 101.4

Table 2. Docking scores of wild-type, G296R, F320S, G321W, E355K, and G401C α IIb β 3 structures.

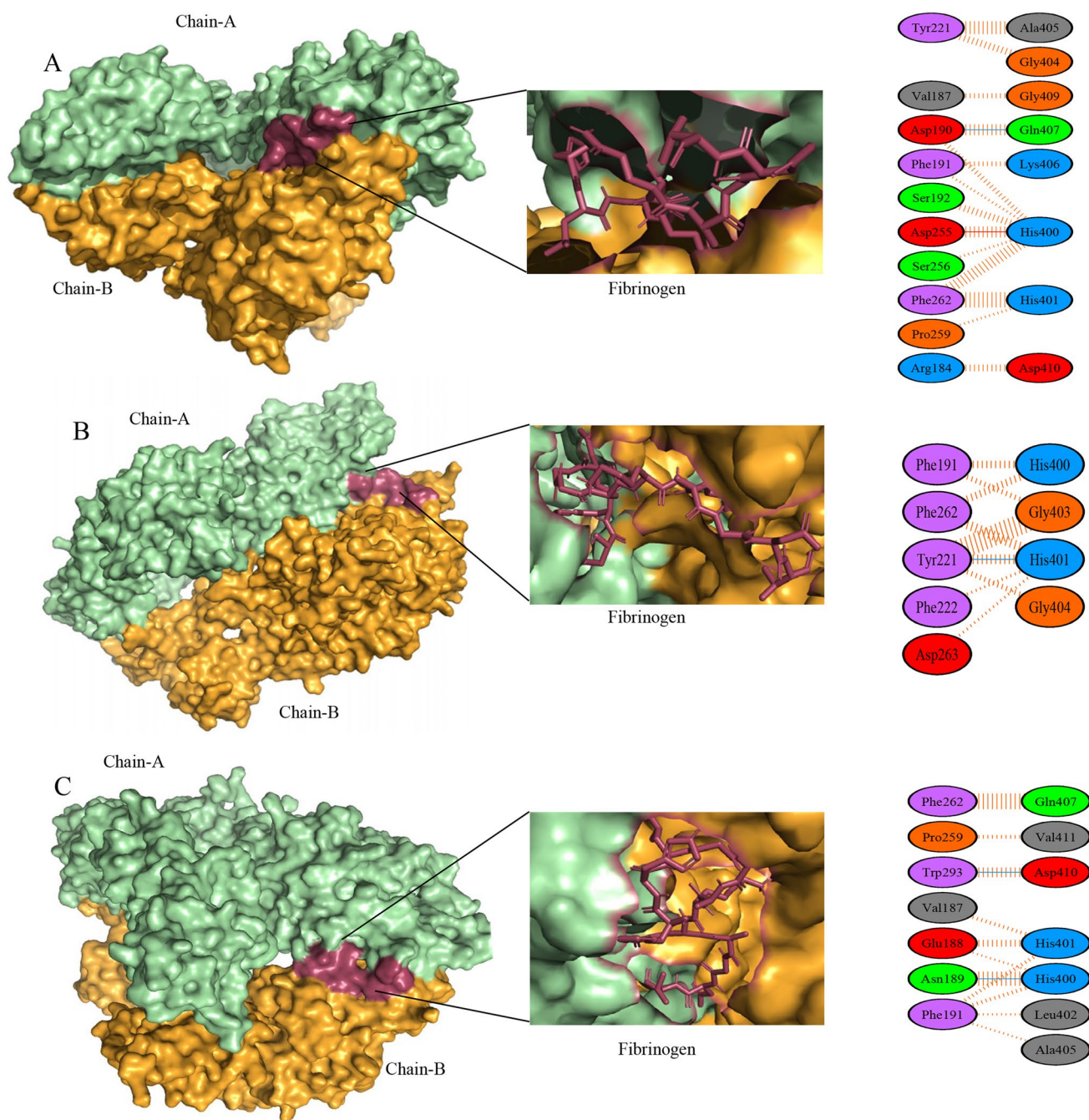


Figure 3. Three dimensional interactions of α IIb β 3 complexes after docking with fibrinogen. Wild-type (A), E355K (B), and G401C (C). Chains A and B represent α IIb and β 3 subunits, respectively.

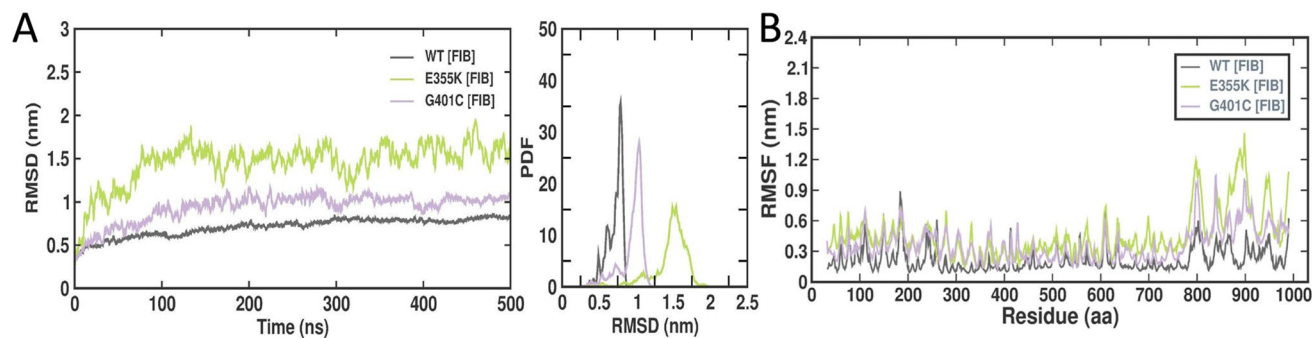


Figure 4. RMSD and RMSF plots of wild-type, E355K, and G401C α IIb β 3 structures bound to fibrinogen following MD simulations (500 ns). (A) RMSD values corresponding to the fibrinogen-bound wild-type, E355K, and G401C α IIb β 3 complexes. The x-axis represents time in ns, while the y-axis represents RMSD values in nm. (B) Graphical representation of RMSF values corresponding to the fibrinogen-bound wild-type, E355K, and G401C α IIb β 3 complexes. The x-axis indicates amino acid residues, while the y-axis indicates RMSF values in nm.

Protein structure	RMSD (nm)	RMSF (nm)	Rg (nm)	SASA (nm ²)
Wild-type	0.71 +/- 0.10	0.22 +/- 0.11	3.79 +/- 0.04	673.33 +/- 29.10
E355K	1.45 +/- 0.25	0.45 +/- 0.22	4.25 +/- 0.09	746.03 +/- 15.69
G401C	0.94 +/- 0.16	0.36 +/- 0.16	4.11 +/- 0.08	718.12 +/- 16.48

Table 3. Average RMSD, RMSF, Rg, and SASA values of fibrinogen-bound wild-type, E355K, and G401C α IIb β 3 complexes.

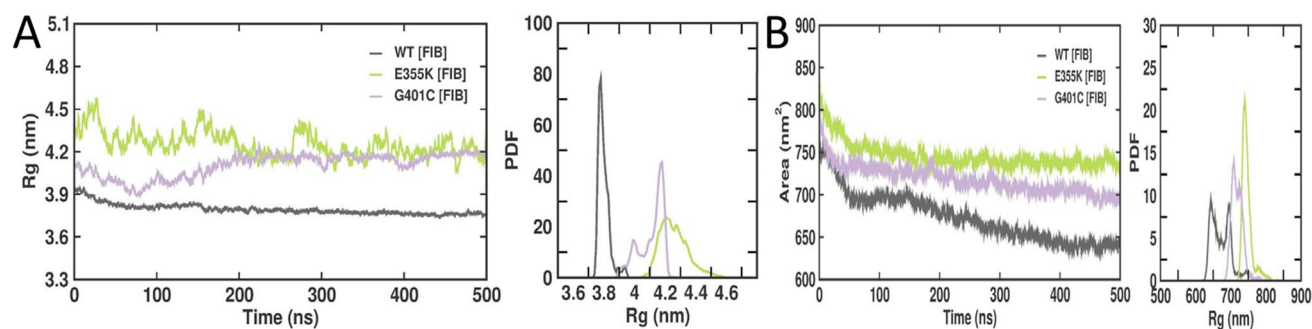


Figure 5. Rg and SASA plots of wild-type, E355K, and G401C α IIb β 3 structures bound to fibrinogen following MD simulations (500 ns). (A) Rg values corresponding to the fibrinogen-bound wild-type, E355K, and G401C α IIb β 3 complexes. The x-axis represents time in ns, while the y-axis represents Rg values in nm. (B) SASA values corresponding to the fibrinogen-bound wild-type, E355K, and G401C α IIb β 3 complexes. The x-axis indicates time in ns, while the y-axis indicates area in nm².

Discussion

The β -propeller domain sits atop integrin α IIb β 3 and is essential for biogenesis, maturation, and ligand binding. N15-linked glycosylation in the β -propeller represents a key quality control step in the biogenesis of α IIb β 3. Mutations in this domain have also been reported to disrupt normal intracellular trafficking by retaining mutant pro- α IIb β 3 complexes in the ER. Ligand binding of α IIb β 3 is mediated by the upper face of the “cap” region owing to the presence of Ca²⁺ and Mg²⁺ ions. In the current study, a total of 177 mutations were retrieved from the databases, such as HGMD, UniProt, ClinVar, and dbSNP, among which 60 were predicted to be deleterious using tools, such as PredictSNP, MAPP, PhD-SNP, Polyphen-1, Polyphen-2, SIFT, and SNAP¹⁷. Based on phenotypic severity, stability changes, and evolutionary conservation status, five mutations, namely G296R, F320S, G321W, E355K, and G401C were studied further by molecular docking analysis of both α IIb with β 3 (protein-protein docking) and α IIb β 3 complex with fibrinogen (protein-peptide docking). Based on their HADDOCK scores, the E355K structure was found to have the lowest binding affinity for fibrinogen followed by the G401C structure indicating that these two mutations might affect α IIb β 3’s ligand binding function, which prompted subsequent MD simulations.

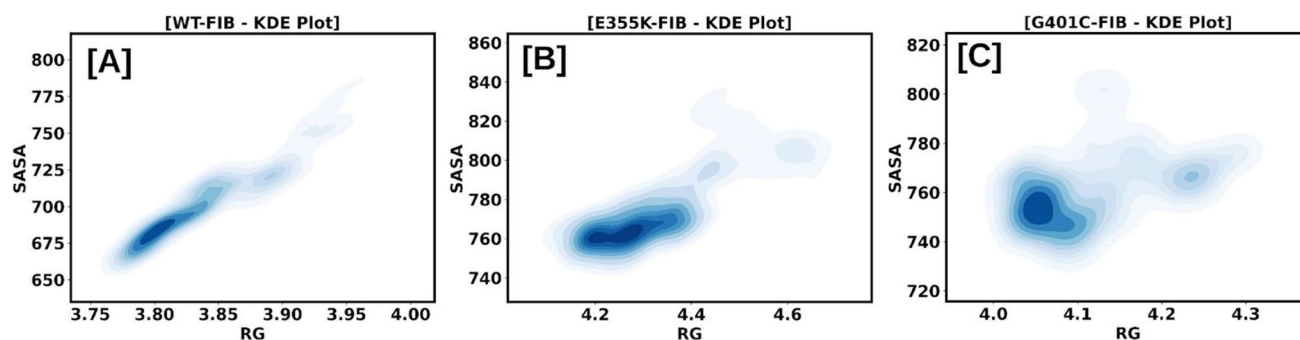


Figure 6. KDE plots of Rg and SASA are represented together as collective variables for fibrinogen-bound wild-type (A), E355K (B), and G401C (C) α IIb β 3 complexes.

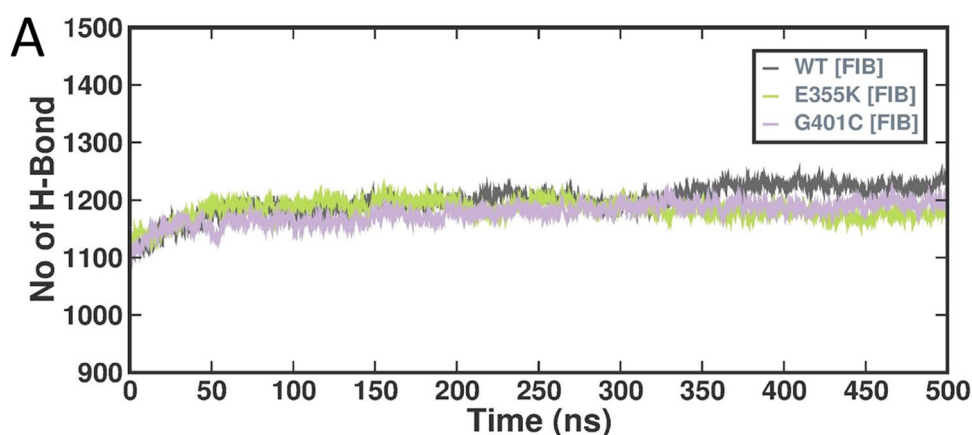


Figure 7. Graphical representations of H-bond interactions of wild-type, E355K, and G401C α IIb β 3 structures bound to fibrinogen following MD simulations (500 ns). The x-axis represents time in ns, while the y-axis represents number of H-bonds.

Protein structure	Total	Coil	β -sheet	β -bridge	Bend	Turn	α -helix	3-helix
Wild-type	50	31	30	3	18	9	7	1
E355K	53	28	32	3	18	10	8	1
G401C	53	28	33	2	18	10	8	1

Table 4. Secondary structure elements in fibrinogen-bound wild-type, E355K, and G401C α IIb β 3 complexes.

The E355K mutation had been maternally inherited by a Swiss patient with GT type 1 (severe phenotype) who was compound heterozygous with a I565T mutation in the α IIb thigh domain which had led to lower α IIb β 3 surface expression^{21,22}. On the other hand, the G401C mutation had been previously reported in a French patient with GT type 2 (moderate phenotype) who was also compound heterozygous with a V934F mutation in the α IIb calf-2 domain²³. Trajectory analysis which includes several parameters, such as RMSD, RMSF, Rg, SASA, SSE, and MMPBSA was carried out for fibrinogen-bound wild-type, E355K, and G401C complexes. RMSD and RMSF showed that the E355K structure showed higher deviations and fluctuations in comparison to both the wild-type and G401C structures. Additionally, fluctuations were observed in the C-terminal residues corresponding to the α IIb calf-2 domain. The average Rg values of the fibrinogen-bound wild-type, E355K, and G401C complexes were 3.83, 4.31, and 4.11 nm, respectively indicating that in contrast to the wild-type structure, both E355K and G401C structures had more deviations thereby compromising their structural stability. Interestingly, the E355K structure had a higher SASA value with an enlarged surface area showing that the structure is not protected from water molecules. Both fibrinogen-bound E355K and G401C complexes displayed a reduced number of hydrogen bonds in comparison to the wild-type. Of note, the G401C mutation had been previously reported to affect the Ca²⁺-binding loop by disrupting hydrogen bonds with neighboring residues²³. Moreover, the average number of secondary structures in both were slightly higher in comparison to the wild-type, particularly β -sheets and α -helices, which could be ascribed to the large size of lysine and cysteine as compared to the respective wild-type residues. As mentioned earlier, the average binding energies for the

A			
Energy (kJ/mol)	Wild-type	E355K	G401C
Van der Waals energy	-171.246 +/-10.092	-224.196 +/- 16.584	-230.061 +/-9.585
Electrostatic energy	-0.145 +/-5.530	-28.530 +/-12.109	-26.105 +/-7.410
Polar solvation energy	69.868 +/-12.438	149.086 +/-35.490	138.083 +/-22.505
SASA energy	-18.322 +/-0.852	-22.691 +/-1.174	-23.408 +/-0.874
Total binding energy	-119.845 +/-11.238	-126.331 +/-22.628	-141.491 +/-17.615
B			
Energy (kJ/mol)	Wild-type	E355K	G401C
Van der Waals energy	-121.87 +/-38.925	-80.56 +/-13.234	-84.43 +/-12.785
Electrostatic energy	-212.475 +/-288.985	-13.363 +/-4.969	-116.754 +/- 12.300
Polar solvation energy	1493.736 +/-293.584	88.872 +/-4.155	213.963 +/-31.597
Hotspot interaction binding energy	-128.661 +/-87.493	-112.925 +/-10.849	-63.998 +/-30.853

Table 5. A. Overall binding energies of fibrinogen-bound wild-type, E355K, and G401C α IIB β 3 complexes. B. Hotspot interaction binding energies of fibrinogen-bound wild-type, E355K, and G401C α IIB β 3 complexes.

E355K and G401C structures were found to be lower when compared to the wild-type structure. However, the hotspot interaction binding energies for these mutant structures were found to be higher than that of the wild-type which explains their absent or reduced fibrinogen binding, respectively²¹. Glutamic acid at the 355th amino acid position which is buried within the β -propeller core is critical for maintaining the domain's structural stability. Hence, substitution with an oppositely charged lysine seemed to have perturbed stability leading to a reduced affinity to bind with fibrinogen. Whereas cysteine substitution of glycine at the 401st position did not bring about substantial changes to the interaction of surrounding residues with fibrinogen binding sites.

In conclusion, our study documents all of the mutations that have been reported so far in the α IIB β -propeller domain. While the E355K mutation has reportedly occurred in a mutation hotspot, the G401C mutation has been reported to disrupt the Ca^{2+} -binding loop. MD simulations revealed that the E355K mutation strongly inhibited complex formation and fibrinogen binding with the G401C mutation having a comparably lesser impact, which could have led to the severe and moderate disease phenotypes in the Swiss and French patients, respectively. Our comprehensive in silico analysis clearly reiterates that mutations in the β -propeller domain may not only be responsible for structural changes in this domain but can also impact the overall structure and function of integrin α IIB β 3. It also provides novel insights into the dynamics of fibrinogen binding with α IIB β 3, which could pave the way for potential diagnostic and targeted therapy for Glanzmann thrombasthenia in the future.

Methods

Retrieval of mutations from databases

Mutations in the ITGA2B gene encoding the α IIB subunit were collected from the databases, like HGMD (www.hgmd.cf.ac.uk)²⁴, Uniprot (www.uniprot.org)²⁵, ClinVar (<https://www.ncbi.nlm.nih.gov/clinvar/>)²⁶, and dbSNP (<https://www.ncbi.nlm.nih.gov/snp/>)²¹. The crystal structure of α IIB β 3 was retrieved from the Protein Data Bank (PDB), which has a resolution of 2.55 Å (PDB ID: 3FCS)¹. The region of interest, namely the β -propeller domain (1-451 residues) was obtained from the α IIB subunit. Human Genome Variation Society (HGVS) nomenclature was followed throughout the study. Furthermore, these mutations were filtered based on various in silico prediction tools.

Pathogenicity and stability analysis

Based on their deleterious nature and their impact on structural stability, the mutations were analyzed and filtered with the help of different tools, such as iStable_SEQ¹⁸, I-mutant_SEQ, MUpro, and CUPSAT using deltaG values and PredictSNP¹⁷ which is an amalgamation of several tools, like PredictSNP, SIFT, Polyphen-1, Polyphen-2, PhD-SNP, SNAP, PANTHER, MAPP, and nsSNPAnalyzer. All these tools were integrated into a consensus classifier to improve their efficiency.

Evolutionary conservation analysis

The conservation of amino acids from an evolutionary standpoint helps correlate the tendency of amino acid(s) to be mutated and the importance of retaining amino acids for functional integrity and structural stability. The ConSurf web server was used for the conservation analysis of amino acid residues bearing mutations at specific sites²⁷.

Protein and ligand preparation

The structure of integrin α IIB β 3 ectodomain determined by X-ray crystallography (PDB: 3FCS) is composed of two globular domains, wherein α IIB and β 3 are separated by a hinge region. Before proceeding with molecular docking, water and other small irrelevant molecules were removed from the structure. The protein receptor was further prepared with the addition of polar compounds and removal of partial charges. The mutations G296R, F320S, G321W, E355K, and G401C were introduced at specific locations in the PyMOL software using in silico

site-directed mutagenesis (www.pymol.org). The fibrinogen structure was extracted from the PubChem database (CID: 90540)²⁸. The ligand binds to the globular domain and the hinge region, which triggers conformational changes on the receptor to regulate its function.

Molecular docking analysis

Molecular docking was performed for select mutations to understand the consequences due to single amino acid substitutions using the HADDOCK software which can determine interactions between protein-protein complexes. HADDOCK allows conformational changes of the molecules during complex formation, for both side chains and the backbone²⁹. Initially, wild-type and mutant structures of α Ib β 3 were analyzed by protein-protein docking between α Ib and β 3 subunits. This helps with identification of ambiguous interaction restraints or active residues. The docking scores were calculated based on intermolecular Van der Waals and electrostatic energies. The complexes with lowest intermolecular energy scores were selected for further analysis. Similarly, protein-peptide docking was done for the wild-type and all five mutant α Ib β 3 complexes in combination with fibrinogen using protein-ligand docking for understanding their interactions with fibrinogen²⁹. The protein-protein and protein-peptide complexes were analyzed using PyMOL software to visualize changes in intermolecular interactions, such as hydrogen bonds and hydrophobic interactions between the wild-type and mutant α Ib β 3 complexes.

Molecular dynamics simulations

The wild-type and mutant α Ib β 3 structures were subjected to molecular dynamics (MD) simulations using GROMOS96 software with 54a7 applied forcefield^{30,31}. The structures of the wild-type and mutants were solvated using Simple Point Charge (SPC) in a cubic box with 1 nm away from its edge. Sodium ions were added for neutralization of the system. Energy minimization of 5000 steps were performed to correct asymmetric geometries by the steepest descent method³². Temperature and pressure were fixed using the Berendsen algorithm with 50,000 ps and 1000 KJ/mol/nm ($T = 300$ K and $P = 1$ bar)³³. The Parrinello-Rahman method was used to normalize temperature and pressure. SETTLE and LINCS algorithms were used to retain the geometry of water molecules and non-water bonds^{19,20}. The wild-type and mutant structures were run for a total simulation time of about 500 ns. MD trajectories, such as root mean square deviation (RMSD), root mean square fluctuation (RMSF), solvent accessible surface area (SASA), radius of gyration (Rg), hydrogen bonds, principal component analysis (PCA), and secondary structure elements (SSE) were all performed using gmx rms, gmx rmsf, gmx sasa, gmx gyrate, gmx hbond and gmx do_dssp. The graphs were plotted using QtGrace software.

Data availability

The datasets generated and/or analyzed during the study have been deposited in BioStudies which can be accessed via the link, <https://doi.org/10.6019/S-BSST1425>.

Received: 21 May 2024; Accepted: 1 October 2024

Published online: 15 October 2024

References

- Zhu, J. et al. Structure of a complete integrin ectodomain in a physiologic resting state and activation and deactivation by Applied forces. *Mol. Cell.* **32**, 849–861 (2008).
- Xiong, J. P. et al. Crystal structure of the extracellular segment of integrin α V β 3 in complex with an arg-gly-asp ligand. *Sci.* (1979). **296**, 151–155 (2002).
- Kiyomizu, K. et al. Recognition of highly restricted regions in the β -propeller domain of α Ib by platelet-associated anti- α Ib β 3 autoantibodies in primary immune thrombocytopenia. *Blood.* **120**, 1499–1509 (2012).
- Westrup, D. et al. Glanzmann Thrombasthenia Frankfurt I is associated with a point mutation Thr176Ile in the N-terminal region of α Ib subunit integrin. *Thromb. Haemost.* **92**, 1040–1051 (2004).
- Mitchell, W. B., Li, J. H., French, D. L. & Collier, B. S. α Ib β 3 biogenesis is controlled by engagement of α Ib in the calnexin cycle via the N15-linked glycan. *Blood.* **107**, 2713 (2006).
- Bray, P. F. et al. Biogenesis of the platelet receptor for fibrinogen: evidence for separate precursors for glycoproteins IIb and IIIa (platelet membrane/fibrinogen receptor/cell-free synthesis/human erythroleukemia cell RNA). *Med. Sci.* **83**, 1480–1484 (1986).
- Poncz, M. et al. Glanzmann Thrombasthenia secondary to a Gly273 \rightarrow asp mutation adjacent to the first calcium-binding domain of platelet glycoprotein IIb. *J. Clin. Invest.* **93**, 172–179 (1994).
- Mitchell, W. B. et al. Two novel mutations in the alpha IIb beta 3 calcium-binding domains identify hydrophobic regions essential for alpha IIb beta 3 biogenesis. *Blood.* **101**, 2268–2276 (2003).
- Wilcox, D. A., Wautier, J. L., Pidard, D. & Newman, P. J. A single amino acid substitution flanking the fourth calcium binding domain of alpha IIb prevents maturation of the alpha IIb beta 3 integrin complex. *J. Biol. Chem.* **269**, 4450–4457 (1994).
- Shen, W. Z. et al. A novel Pro126His β propeller mutation in integrin α Ib causes Glanzmann Thrombasthenia by impairing progression of pro- α Ib β 3 from endoplasmic reticulum to Golgi. *Blood Cells Mol. Dis.* **42**, 44–50 (2009).
- Rosenberg, N.*., Landau, M., Luboshitz, J. &*, Rechavi, G. Seligsohn U. A novel Phe171Cys mutation in integrin α Ib causes Glanzmann Thrombasthenia by abrogating α Ib β 3 complex formation. *J. Thromb. Haemost.* **2**, 1167–1175 (2002).
- Nelson, E. et al. Three novel β -propeller mutations causing Glanzmann Thrombasthenia result in production of normally stable pro- α IIb, but variably impaired progression of pro- α IIb β 3 from endoplasmic reticulum to Golgi. *J. Thromb. Haemost.* **3**, 2773–2883 (2005).
- Chandrasekaran, F. P. et al. Molecular dynamics simulations corroborate recombinant expression studies carried out on three α Ib β -propeller mutations reported in Indian Glanzmann Thrombasthenia patients. *J. Cell. Biochem.* **124**, 989–1001 (2023).
- Springer, T. A., Zhu, J. & Xiao, T. Structural basis for distinctive recognition of fibrinogen γ C peptide by the platelet integrin α Ib β 3. *J. Cell Biol.* **182**, 791–800 (2008).
- Xiao, T., Takagi, J., Collier, B. S., Wang, J. H. & Springer, T. A. *Structural Basis for allostery in integrins and binding to fibrinogen-mimetic therapeutics.* www.nature.com/nature (2004).
- Kamata, T., Tieu, K. K., Irie, A., Springer, T. A. & Takada, Y. Amino acid residues in the α Ib Subunit that are critical for Ligand binding to integrin α Ib β 3 are clustered in the β -Propeller model. *J. Biol. Chem.* **276**, 44275–44283 (2001).

17. Bendl, J. et al. PredictSNP: robust and accurate consensus classifier for prediction of disease-related mutations. *PLoS Comput. Biol.* **10**, e1003440 (2014).
18. Chen, C. W., Lin, M. H., Liao, C. C., Chang, H. P. & Chu, Y. W. iStable 2.0: Predicting protein thermal stability changes by integrating various characteristic modules. *Comput. Struct. Biotechnol. J.* **18**, 622–630 (2020).
19. Hess, B., Bekker, H., Berendsen, H. J. C. & Fraaije, J. G. E. M. LINCS: a linear constraint solver for molecular simulations. *J. Comput. Chem.* **18**, 14631472 (1997).
20. Miyamoto, S. & Kollman, P. A. Settle: an analytical version of the SHAKE and RATTLE algorithm for rigid water models. *J. Comput. Chem.* **13**, 952–962 (1992).
21. French, D. L. & Collier, B. S. *Hematologically important mutations: glanzmann thrombasthenia.* (1997).
22. Ruan, J. Double heterozygosity of the GPIIb gene in a swiss patient with Glanzmann's thrombasthenia. *Br J Haematol.* **102**, 18–25 (1998).
23. Nurden, A. T. et al. Expanding the mutation spectrum affecting α IIb β 3 integrin in glanzmann thrombasthenia: screening of the ITGA2B and ITGB3 genes in a large International Cohort. *Hum. Mutat.* **36**, 548–561 (2015).
24. Stenson, P. D. et al. The human gene mutation database (HGMD): optimizing its use in a clinical diagnostic or research setting. *Hum. Genet.* **139**, 1197–1207 (2020).
25. Bateman, A. et al. UniProt: the Universal protein knowledgebase in 2023. *Nucleic Acids Res.* **51**, D523–D531 (2023).
26. Landrum, M. J. et al. ClinVar: improvements to accessing data. *Nucleic Acids Res.* **48**, D835–D844 (2020).
27. Ben Chorin, A. et al. ConSurf-DB: an accessible repository for the evolutionary conservation patterns of the majority of PDB proteins. *Protein Sci.* **29**, 258–267 (2020).
28. Kim, S. et al. PubChem substance and compound databases. *Nucleic Acids Res.* **44**, D1202 (2016).
29. Dominguez, C., Boelens, R. & Bonvin, A. M. J. HADDOCK: a protein-protein docking approach based on biochemical or biophysical information. *J. Am. Chem. Soc.* **125**, 1731–1737 (2003).
30. Abraham, M. J. et al. GROMACS: high performance molecular simulations through multi-level parallelism from laptops to supercomputers. *SoftwareX* **1**, 19–25 (2015).
31. Schmid, N. et al. Definition and testing of the GROMOS force-field versions 54A7 and 54B7. *Eur. Biophys. J.* **2011**, **40**:7 **40**, 843–856 (2011).
32. Petrova, S. S. & Solov'Ev, A. D. The origin of the method of steepest descent. *Historia Math.* **24**, 361–375 (1997).
33. Berendsen, H. J. C., Postma, J. P. M., van Gunsteren, W. F. & Hermans, J. Interaction models for water in relation to protein hydration. *Intermolecular Forces* **14**, 331–342 (1981).

Author contributions

FPC designed the study, collected and analyzed the data, interpreted the results, and drafted the manuscript. EJRN conceptualized and supervised the study, interpreted the results, and critically reviewed and edited the manuscript.

Declarations

Competing interests

The authors declare no competing interests.

Additional information

Supplementary Information The online version contains supplementary material available at <https://doi.org/10.1038/s41598-024-75070-4>.

Correspondence and requests for materials should be addressed to E.J.R.N.

Reprints and permissions information is available at www.nature.com/reprints.

Publisher's note Springer Nature remains neutral with regard to jurisdictional claims in published maps and institutional affiliations.

Open Access This article is licensed under a Creative Commons Attribution-NonCommercial-NoDerivatives 4.0 International License, which permits any non-commercial use, sharing, distribution and reproduction in any medium or format, as long as you give appropriate credit to the original author(s) and the source, provide a link to the Creative Commons licence, and indicate if you modified the licensed material. You do not have permission under this licence to share adapted material derived from this article or parts of it. The images or other third party material in this article are included in the article's Creative Commons licence, unless indicated otherwise in a credit line to the material. If material is not included in the article's Creative Commons licence and your intended use is not permitted by statutory regulation or exceeds the permitted use, you will need to obtain permission directly from the copyright holder. To view a copy of this licence, visit <http://creativecommons.org/licenses/by-nc-nd/4.0/>.

© The Author(s) 2024